

**“BABEȘ-BOLYAI” UNIVERSITY
FACULTY OF PHYSICS**

STĂNESCU RAMONA

**STRUCTURAL STUDIES OF SOME OXIDE
VITREOUS SYSTEMS WITH TRANSITIONAL
METAL IONS**

Ph. D Thesis Summary

**SCIENTIFIC SUPERVISOR
PROF. UNIV. DR. ONUC COZAR**

**CLUJ-NAPOCA
2014**

CONTENTS

Thesis

INTRODUCTION	5
CHAPTER 1. VITREOUS OXIDE MATERIALS	
1.1. General aspects related to the structure of vitreous oxide materials.....	9
1.2. Network former and modifier oxides.....	11
1.3. Methods used in the oxide glasses preparation	12
1.4. The crystalline and vitreous structure of P_2O_5	14
1.5. Binary glasses based on P_2O_5	17
1.6. Applications of phosphate glasses.....	21
CHAPTER 2. METHODS USED IN THE STUDY OF VITREOUS OXIDE MATERIALS	
STRUCTURE	
2.1. Vibrational spectroscopy.....	23
2.1.1. IR absorption spectroscopy.....	23
2.1.2. Vibration types.....	26
2.1.3. Raman spectroscopy.....	28
2.1.4. IR and Raman applications of phosphate glasses.....	33
2.2. Electronic paramagnetic resonance (EPR) spectroscopy.....	36
2.2.1. The basic principles of EPR.....	36
2.2.2. Hyperfine structure (hfs).....	42
2.2.3. The vanadyl ions (VO^{2+}) structure.....	45
2.2.4. The results obtained using EPR on phosphate glasses with vanadium (V^{4+}).....	50
2.3. Thermoluminescence of the phosphate glasses	54
2.3.1. Thermoluminescence phenomena.....	54
2.3.2. Thermoluminescence of some materials.....	58
2.3.3. Thermoluminescence of phosphate glasses.....	59
CHAPTER 3. STRUCTURAL STUDIES OF $V_2O_5 - P_2O_5 - BaO$ GLASS SYSTEM	
3.1. Sample preparation.....	62
3.2. IR study of $xV_2O_5(100-x)[0.8P_2O_5 \cdot 0.2BaO]$ glass system.....	64
3.3. Raman study of $xV_2O_5(100-x)[0.8P_2O_5 \cdot 0.2BaO]$ glass system.....	70

3.4. EPR study of $xV_2O_5(100-x)[0.8P_2O_5 \cdot 0.2BaO]$ glass system.....	76
Conclusions.....	81
CHAPTER 4. STRUCTURAL STUDIES OF $V_2O_5 - P_2O_5 - Bi_2O_3$ GLASS SYSTEM	
4.1. $xV_2O_5(100-x)[0.8P_2O_5 \cdot 0.2Bi_2O_3]$ glass system.....	82
4.1.1. Sample preparation.....	82
4.1.2. IR study of $xV_2O_5(100-x)[0.8P_2O_5 \cdot 0.2Bi_2O_3]$ glass system.....	84
4.1.3. Raman study of $xV_2O_5(100-x)[0.8P_2O_5 \cdot 0.2Bi_2O_3]$ glass system.....	88
4.1.4. EPR study of $xV_2O_5(100-x)[0.8P_2O_5 \cdot 0.2Bi_2O_3]$ glass system.....	94
4.2. $xV_2O_5(100-x)[0.5P_2O_5 \cdot 0.5Bi_2O_3]$ glass system.....	98
4.2.1. Sample preparation.....	98
4.2.2. IR study of $xV_2O_5(100-x)[0.5P_2O_5 \cdot 0.5Bi_2O_3]$ glass system.....	99
4.2.3. Raman study of $xV_2O_5(100-x)[0.5P_2O_5 \cdot 0.5Bi_2O_3]$ glass system.....	104
4.2.4. EPR study of $xV_2O_5(100-x)[0.5P_2O_5 \cdot 0.5Bi_2O_3]$ glass system.....	107
Conclusions.....	109
CHAPTER 5. $V_2O_5 - P_2O_5 - K_2O$ GLASS SYSTEM. ANTIBACTERIAL EFFECT	
5.1. Sample preparation.....	111
5.2. IR study of $xV_2O_5(100-x)[0.8P_2O_5 \cdot 0.2K_2O]$ glass system.....	113
5.3. EPR study of $xV_2O_5(100-x)[0.8P_2O_5 \cdot 0.2K_2O]$ glass system.....	116
5.4. Antibacterial effect study of $xV_2O_5(100-x)[0.8P_2O_5 \cdot 0.2K_2O]$ glass system.....	122
Conclusions.....	125
CHAPTER 6. $P_2O_5 - BaO - K_2O$ GLASS SYSTEM. THERMOLUMINESCENCE PROPERTIES	
6.1. Sample preparation.....	126
6.2. IR study of $0.5P_2O_5 - xBaO - (0.5-x)K_2O$ glass system.....	127
6.3. Raman study of $0.5P_2O_5 - xBaO - (0.5-x)K_2O$ glass system.....	130
6.4. Thermoluminescence study of $0.5P_2O_5 - xBaO - (0.5-x)K_2O$ glass system.....	133
Conclusions.....	138
GENERAL CONCLUSIONS.....	139
REFERENCES.....	142

INTRODUCTION

Keywords: phosphate glasses, transitional metal (TM) ions, IR spectroscopy, Raman spectroscopy, electron paramagnetic resonance (EPR), thermoluminescence (TL) phenomena, antibacterial effect.

The interest for the investigation of vitreous oxide materials was stimulated by the many applications of these materials in the different fields of science and technique. Nowadays, the study of vitreous oxide materials represents a special field in the larger field of the material science.

Phosphate glasses, a special group of oxide materials, are studied because of a great variety of applications in the field of: physics of semiconductors, optical devices, lasers, magnetic materials, biomaterials as well as nuclear waste hosts.

The addition of transitional metal (TM) ions leads to the depolymerization of the phosphate chains and to the formation of new P – O – TM linkages, which can change the electrical, optical or magnetic properties of these types of glasses.

The aim of the present PhD thesis was to obtain new experimental data on the structure of phosphate glasses doped with vanadium ions. The thesis also tries to obtain new information about the thermoluminescence of these types of glasses as well as their possible antibacterial activity.

Chapter 1 presents some theoretical aspects for obtaining and structural characterizing the oxide glasses, especially phosphate glasses, as well as its practical importance.

Chapter 2 describes different complementary methods used in their investigation: IR, Raman and EPR spectroscopy and also thermoluminescence phenomena. The theoretical aspects were completed with some experimental data, from the specific field, to illustrate the practical importance of these studies.

Chapter 3 presents the results obtained in IR, Raman and EPR study of $xV_2O_5(100-x)[0.8P_2O_5 \cdot 0.2BaO]$ glass system, with $0 \leq x \leq 50\%$ mol. It is also described the experimental equipment for IR measurements. These results emphasize the local symmetry of the vanadium ions in the studied types of glasses, but also the network modifier role for low content of V_2O_5 and network former role for high content of V_2O_5 .

Chapter 4 presents the results obtained in IR, Raman and EPR study of $xV_2O_5(100-x)[0.8P_2O_5 \cdot 0.2Bi_2O_3]$ and $xV_2O_5(100-x)[0.5P_2O_5 \cdot 0.5Bi_2O_3]$ glass systems, with $0 \leq x \leq 50\%$ mol. It is also described the experimental equipment for Raman measurements. Both P_2O_5 and Bi_2O_3 oxides of the investigated glasses are known as network formers, but Bi_2O_3 is an unconventional one. In the same time, it was observed a competition between Bi_2O_3 and P_2O_5 , as classical former oxides on one side and the network modifier V_2O_5 , on the other side. Both Bi_2O_3 and P_2O_5 are network former oxides, but P_2O_5 forms more organized long range structures than Bi_2O_3 . These results underline the dual role of V_2O_5 , as network modifier and former, induced by V_2O_5 content.

Chapter 5 presents the results obtained in IR and EPR study of $xV_2O_5(100-x)[0.8P_2O_5 \cdot 0.2K_2O]$ glass system, with $0 \leq x \leq 50\%$ mol. In addition, the antibacterial effect of the investigated glasses was tested. It is also described the experimental equipment for EPR measurements. The same dual role of vanadium oxide is also proved by the investigated types of glasses; the antibacterial activity of the investigated system presents the same tendency for both Gram-positive (*S. aureus*) and Gram-negative (*E. coli*) strains.

Chapter 6 presents the results obtained with IR, Raman and thermoluminescence phenomena study of $0.5 P_2O_5 - xBaO - (0.5-x) K_2O$ glass system, with $0 \leq x \leq 0.5$. It is also described the experimental equipment for thermoluminescence measurements. The thermoluminescence studies of the investigated glass system show that both Ba^{2+} and K^+ modifier oxides generated thermoluminescence phenomena.

Bibliography cited is specific theme addressed, using the latest scientific results in the field.

CHAPTER 1

VITREOUS OXIDE MATERIALS

Non – crystalline solids represent those materials in which the atoms are very close situated to each other like in the crystals, but their arrangement is an irregular one. Such non – crystalline solids can be glasses or other amorphous materials, without a clear delimitation between them.

Vitreous state notion which is used to define the glass structure is a restricted one, in the way that there is only a local (short range) order between the atoms.

The basic oxide which is dominant at the molecular structure level of the glass, called vitreous network former, has a decisive role in making the structural framing of the glass. The other oxides which enter in the composition of the glass have no contribution to the structural framing, but they stabilize its random structure, are called modifiers or stabilizers of the vitreous network.

The most commonly used method of obtaining oxide materials with a vitreous structure is that of melt-quenching. Oxide materials with vitreous structure can also be obtained using the mechanical energy, the action of the neutrons, the sol-gel method as well as the coating of thin layers on cold surfaces.

Phosphate glasses have been studied mainly because of their interesting optical, thermal and magnetic properties and in consequence for their potential applications.

The study of phosphate glasses requires a detailed understanding in order to help the determination of relationship between physical properties and their structural units.

Vitreous phosphate network is based on PO_4 tetrahedra (Fig.1), each of them sharing three corners. The tetrahedra are linked to three other tetrahedra through bridging P – O – P oxygen atoms. The fourth bond is linked to a terminal oxygen atom (P = O bonds) and it is significantly shorter than the others, the fourth being in the same time inactive from the chemical point of view.

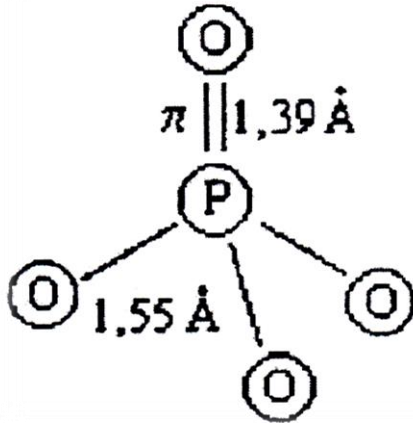


Fig. 1. PO₄ molecular formula

In consequence, the network of phosphate glasses contains a polymeric structure. The addition of TM oxides leads to the depolymerization of the phosphate chains and to the formation of new P – O – TM linkages.

The structure of binary phosphate glasses are described with the so-called Qⁿ group model. The phosphate structural groups pass from Q³ to Q² to Q¹ to Q⁰ as the ratio M₂O/P₂O₅ = R passes from 0 to 1, 2 and finally to 3.

Phosphate glasses are known as materials for optoelectronics because of their several unique properties, such as: high refractive index, low melting point, low viscosity, present UV transmission and present electrical conduction. The electrical properties of the phosphate glasses can be improved by controlled doping with TM ions. From this point of view, phosphate glasses doped with vanadium ions have received special attention due to their semiconducting properties and electrical conduction which occurs via polaron hopping between V⁴⁺ and V⁵⁺ centers.

Phosphate glasses are used with great success for several optical applications: for camera lenses designed to transmit UV light or for fiber optics designed as light conductors. Some phosphate glasses are photosensible and can be used to obtain good quality images. They are also used for holograms, as filters for different optical radiations or for microsystems used to encapsulate sensors or other optoelectronic devices. Phosphate glasses containing Ag⁺, Cu⁺ or Zn⁺ are studied for their potential application as antibacterial materials. Metal ions such as cobalt and vanadium and their complexes are found to be antitumor active, catalytic active, antimicrobial and cytotoxic.

CHAPTER 2

METHODS USED IN THE STUDY OF VITREOUS OXIDE MATERIALS STRUCTURE

A lot of classical methods are suitable for the study of the phosphate glasses. The present work describes some of them: IR and Raman spectroscopy, electron paramagnetic resonance (EPR) spectroscopy and thermoluminescence (TL) phenomena.

By analyzing the transitions between the vibration and vibration – rotation level, IR and Raman spectroscopy can provide important information about molecular dynamics for crystalline and non – crystalline substances.

There are some common features of the vibration spectra of the glasses:

1. IR and Raman bands are larger than those belonging to the crystals;
2. Although they are large, they are also symmetrical;
3. The number of the bands varies from 1 to 3 per each unit.

Regarding the vitreous systems, EPR gives precise and direct information about the glass microstructure. Nowadays, EPR spectroscopy is used to identify the paramagnetic centers, the local symmetry of some ions, the fundamental state, the influence of the neighbors on the paramagnetic center and for the calculation of crystal field parameters. EPR also allows the detection of the TM ions, the confirmation of the valence state of ions and the ion – network interaction intensity.

The thermoluminescent materials are able to store the energy of ionizing radiation and convert this energy into electromagnetic (light) radiation under the influence of thermal radiation. The most used materials in thermoluminescence dosimeters are insulators and semiconductors. One of the objectives of thermoluminescence measurements is to extract the data from the „glow curve” and to use them in order to calculate the values of different parameters associated to the charge transfer process which takes place in the analyzed material.

TL glass dosimeters are of particular interest due to their outstanding properties such as their good thermal stability, having a tissue equivalent identity, relatively low cost, easily shaped, good ability to host luminescent activators in elevated concentrations and an increasing possibility of providing optical fibers that are used in manufacturing bidimensional detectors.

In the present work, the method used for obtaining oxide materials with a vitreous structure is that of melt-quenching. All the oxides used have the analytical high grade purity. The

samples were prepared by weighting suitable amounts of each component, powder mixing and mixture melting in sintered corundum crucibles. The temperature and time for melting have been chosen taking into account the decomposing and melting temperatures of the components that are to be found in the mixture of the samples. The melted glasses were cooled at room temperature by quickly pouring into stainless steel plates. Because these glasses are hygroscopic, the obtained samples were kept into the exicator surrounded by silicagel.

The structure of samples was analyzed by means of X-ray diffraction, using a Bruker D8 Advanced X-ray diffractometer with a graphite monochromator for CuK_α radiation, with $\lambda = 1.54\text{\AA}$. The pattern obtained did not reveal any crystalline phase in all samples.

IR spectra were recorded with a Bruker Equinox 55 spectrometer, in $400\text{--}2000\text{ cm}^{-1}$, using the anhydrous KBr technique, for avoid structural modifications caused by the ambient moisture. The resolution of the IR spectra is of 2 cm^{-1} .

Raman spectra was recorded, on bulk samples, at room temperature, using an integrated FRA 106 – S Raman module attached to Bruker Equinox 55 spectrometer. The spectral resolution was about 4 cm^{-1} .

EPR measurements were performed at 9.4 GHz (X-band), at room temperature, using ADANI Portable PS8400 equipment.

Thermoluminescence measurements were performed on Risø TL/OSL-DA-20 reader. All luminescence emissions were detected with a bialkali EMI 9235QA photomultiplier tube using a Hoya U-340 filter (transmission between 290 and 390 nm). Irradiations were carried out at room temperature using automatically in the luminescence reader a $^{90}\text{Sr} - ^{90}\text{Y}$ beta source with a dose rate of 0.05 Gy/s .

CHAPTER 3

STRUCTURAL STUDIES OF $V_2O_5 - P_2O_5 - BaO$ GLASS SYSTEM

$xV_2O_5(100-x)[0.8P_2O_5 \cdot 0.2BaO]$ glass system, with $0 \leq x \leq 50\%$ mol, was prepared and investigated. High purity $(NH_4)_2HPO_4$, $BaCO_3$ și V_2O_5 powders were used as starting materials; melting temperature: $1250^\circ C$; time of melting: 5 min.

IR study of $xV_2O_5(100-x)[0.8P_2O_5 \cdot 0.2BaO]$ glass system

IR spectra for $xV_2O_5(100-x)[0.8P_2O_5 \cdot 0.2BaO]$ glass system, with $0 \leq x \leq 50\%$ mol, are given in figure 2.

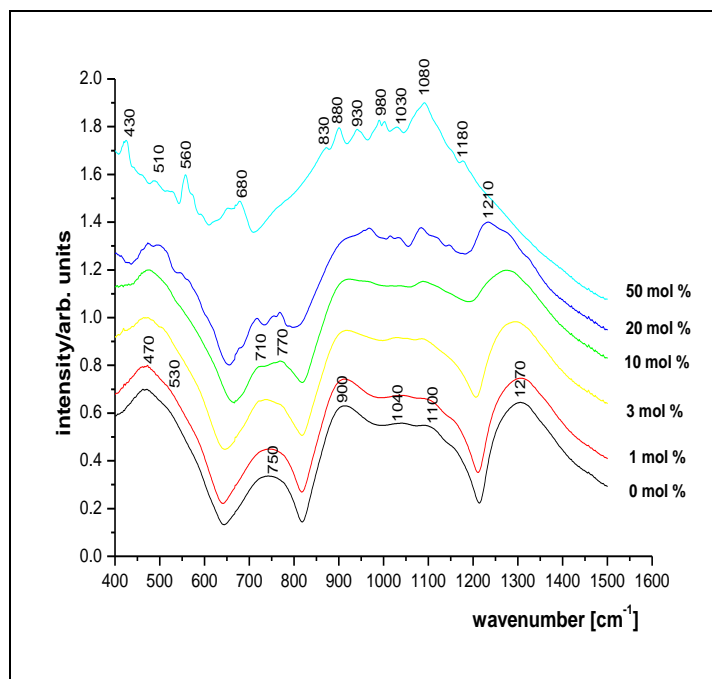


Fig. 2. IR spectra of $xV_2O_5(100-x)[0.8P_2O_5 \cdot 0.2BaO]$ glass system

The specific IR bands for phosphate network ($x = 0$ mol%) are situated in the following regions: ~ 500 cm^{-1} , ~ 750 cm^{-1} , $\sim 900 - 1150$ cm^{-1} și ~ 1270 cm^{-1} . The low wavenumber envelope (~ 500 cm^{-1}) consists of two component bands: the first band (~ 470 cm^{-1}) is assigned to the bending vibrations of O – P – O units and the second band (~ 530 cm^{-1}) to harmonics of bending vibrations of O = P – O linkages. The band from ~ 750 cm^{-1} may be attributed to the symmetric stretching vibrations of the P – O – P linkages; the absorption band situated at

$\sim 900 \text{ cm}^{-1}$ is assigned to the asymmetric stretching modes of P – O – P linkages in linear metaphosphate chain. The weak bands near $\sim 1040 \text{ cm}^{-1}$ and $\sim 1100 \text{ cm}^{-1}$ may be attributed to PO_3^{2-} end groups and to P – O⁻ groups (chain terminator), respectively. The band near $\sim 1270 \text{ cm}^{-1}$ is attributed to the asymmetric stretching mode of the doubly bonded oxygen vibrations P = O.

The shape of the spectra is changing with increase of the V_2O_5 oxide content. New and better evidenced bands appear in the $\sim 710 - 770 \text{ cm}^{-1}$ range, which may be attributed to symmetric stretching vibrations of P – O – P rings and PO_4^{3-} stretching vibrations, respectively. For the same concentration range ($x < 20\%$ mol), the band at $\sim 900 \text{ cm}^{-1}$ is attenuated due to the breaking of P – O – P chains in Q^1 groups and thus to increasing the disorder degree in the phosphate network.

The most noticeable change with the increase of V_2O_5 content is at $\sim 1270 \text{ cm}^{-1}$ band, which decreases in amplitude and shifts to lower wave numbers ($\sim 1210 \text{ cm}^{-1}$), for $x = 20\%$ mol. This fact suggests that V_2O_5 acts in this concentration range as a network former.

For higher content of vanadium ions ($x \geq 20\%$ mol) the bands at $\sim 880 \text{ cm}^{-1}$, $\sim 930 \text{ cm}^{-1}$, $\sim 980 \text{ cm}^{-1}$, $\sim 1080 \text{ cm}^{-1}$ and $\sim 1180 \text{ cm}^{-1}$ dominate the spectrum in the high wavenumber region, and the $\sim 430 \text{ cm}^{-1}$, $\sim 510 \text{ cm}^{-1}$, $\sim 560 \text{ cm}^{-1}$ and $\sim 680 \text{ cm}^{-1}$, in the low wavenumber region. Finally, at $x = 50 \text{ mol}\%$ the bands characteristic to phosphate network are strongly attenuated in intensity, except those specific for short chains units (ring structures) and the bands specific for vanadium oxide become more intense, dominating the IR spectrum.

The bands in $\sim 430 - 680 \text{ cm}^{-1}$ range are due to the lattice vibrations in vanadium oxide network. The $\sim 830 \text{ cm}^{-1}$ band appears from the bridge vibrations of the V – O – V chains of the lattice, while the broad absorption from $\sim 1080 \text{ cm}^{-1}$ is due to the vibrations of the isolated V = O vanadyl groups in VO_5 trigonal bipyramids. The band at $\sim 880 \text{ cm}^{-1}$ may be assigned to the symmetric vibration of the V – O bonds of the VO_4 tetrahedra in glass structure. The other bands from $\sim 930 \text{ cm}^{-1}$ to $\sim 1030 \text{ cm}^{-1}$ may be attributed to V – O bonds and also to the polyvanadate (clustered) ions formations.

So, we may finally conclude that vanadium atoms bridge with non-bridging oxygen of PO_4 units and V_2O_5 oxide acts as a network former for high concentration ($x \geq 20\%$ mol).

Raman study of $xV_2O_5(100-x)[0.8P_2O_5 \cdot 0.2BaO]$ glass system

Raman spectra of the phosphate matrix and low content of V_2O_5 ($0 < x < 0.5$ % mol) show typical bands specific to the phosphate network.

Similar with the results obtained from IR spectra of the studied glass system, Raman spectra shows the same tendency of network depolymerization with increase of V_2O_5 content.

For $x = 5\%$ mol, Raman spectra presents already major changes compared with the spectra corresponding for low V_2O_5 concentration. New bands appears in the spectrum: the bands at $\sim 500\text{ cm}^{-1}$ are assigning to vibrations of $V - O - V$ chains; the band at $\sim 850\text{ cm}^{-1}$ is ascribed to a combination of various vibrations of oxygen bridging within $V - O - V$, $P - O - P$ and $V - O - P$ linkages; the bands in the range $\sim 960\text{ cm}^{-1}$ are assigned to $V = O$ vibrations within the VO_5 tetragonal pyramid and the band at $\sim 1130\text{ cm}^{-1}$ is attributed to PO_2^- “strained” structures.

For high content of V_2O_5 ($x = 50\text{ mol}\%$), all the bands specific for vanadium ($\sim 500\text{ cm}^{-1}$, $\sim 830\text{ cm}^{-1}$, $\sim 960\text{ cm}^{-1}$ and $\sim 1050\text{ cm}^{-1}$) increase in intensity and dominate the spectrum (Fig. 3).

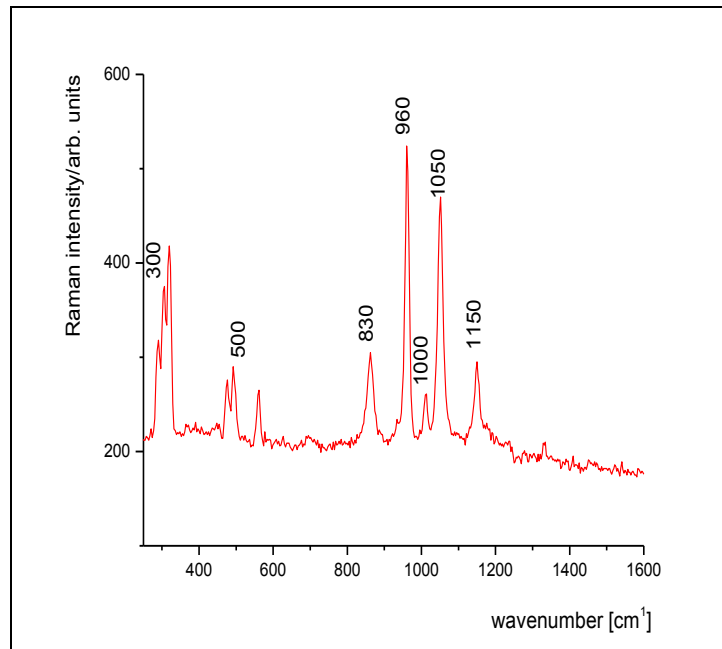


Fig. 3. Raman spectra of $xV_2O_5(100-x)[0.8P_2O_5 \cdot 0.2BaO]$ glasses, with $x = 50\%$ mol

Both IR and Raman studies show that up to $x = 10\%$ mol, V_2O_5 acts as phosphate network modifier. The depolymerization process induced by the addition of V_2O_5 content reduces the bonding force between P and O atoms and produces the appearance of more non-bonding oxygen ions that are involved then in new V – O – V bonds. Finally, the phosphate groups are isolated in the vanadate network and, in consequence, V_2O_5 acts for $x \geq 20\%$ mol as a network former instead of a network modifier.

EPR study of $xV_2O_5(100-x)[0.8P_2O_5 \cdot 0.2BaO]$ glass system

Representative EPR spectra for $xV_2O_5(100-x)[0.8P_2O_5 \cdot 0.2BaO]$ glass system are given in figure 4.

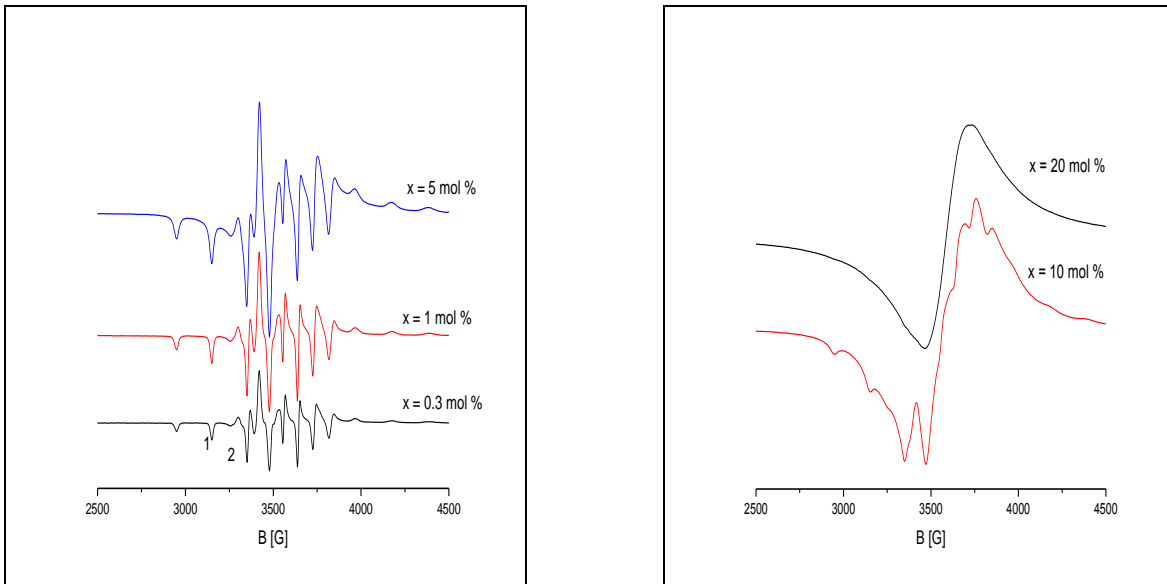


Fig. 4. EPR spectra of $xV_2O_5(100-x)[0.8P_2O_5 \cdot 0.2BaO]$ glass system

For low content of V_2O_5 ($x < 10\%$ mol), these spectra show a well resolved the eight hyperfine (hfs) lines in both parallel and perpendicular bands, typical for unpaired $3d^1$ electron of VO^{2+} ion associated with ^{51}V ($I = 7/2$) isotope in an axially symmetric crystal field. At high content of vanadium oxide ($x \geq 10\%$ mol), the EPR spectra may be regarded as a superposition of two EPR signals, one with a well resolved hfs, typical for isolated VO^{2+} ions and another one consisting in a broad line typical for associated (clustered) V^{4+} ions.

The g and A values obtained in the present work (Table 1) agree with reported by other authors, showing that $g_{\parallel} < g_{\perp} < g_e$ și $A_{\parallel} > A_{\perp}$, relations that correspond to vanadyl ions in square pyramidal site as C_{4v} symmetry. The value estimated for K (~ 0.84) (Table 1) indicates a poor contribution of the vanadium $4s$ orbital to the vanadyl bond in these glasses. The dipolar hyperfine coupling parameter value P ($\sim 139 \cdot 10^{-4} \text{ cm}^{-1}$) (Tab. 1) is similar with that reported for other phosphate glasses containing vanadium ions. The MO coefficients (Table 1) show a ionic character for both π bonds in xOy base-pyramidal plane ($\beta_2^2 \cong 1$) and with vanadyl oxygen ($\varepsilon_{\pi}^2 \cong 0.91$).

Table 1. EPR parameters and MO coefficients for $xV_2O_5(100-x)[0.8P_2O_5 \cdot 0.2BaO]$ glass system*

x mol%	g_{\parallel}	g_{\perp}	A_{\parallel} 10^{-4} cm^{-1}	A_{\perp} 10^{-4} cm^{-1}	K	P 10^{-4} cm^{-1}	β_2^2	ε_{π}^2
0.3	1.94	1.98	197	77	0.84	139	1.04	0.91
0.5	1.92	2.00	195	78	0.85	137	1.08	0.91
1	1.93	1.99	197	79	0.86	138	1.15	0.91
3	1.92	2.00	197	78	0.84	139	1.08	0.90
5	1.92	2.00	198	77	0.83	141	1.14	0.90

*The error on g values is 0.01 and $1 \cdot 10^{-4} \text{ cm}^{-1}$ on the A values.

The dipole–dipole interactions prevail between V^{4+} ions in the composition range of $x < 10\%$ mol. This fact is suggested by the composition dependence of the line-width of first ΔB_1 and second ΔB_2 hfs-peaks from the parallel absorption (Fig. 5.a.), which increase with V_2O_5 content, proving the diminution of $V^{4+} - V^{4+}$ distance. This is possible due to the depolymerization process induced by V_2O_5 in phosphate matrix and thus its network modifier role.

For $x \geq 20\%$ mol, ΔB of the broad line decreases with the increasing of V_2O_5 content due to the presence of superexchange interaction in $V^{4+} - O^{2-} - V^{4+}$ chains (Fig. 5.b.). The presence of vanadate structures which isolate the phosphate groups at high V_2O_5 content is in accord with the network former role of this metallic oxide.

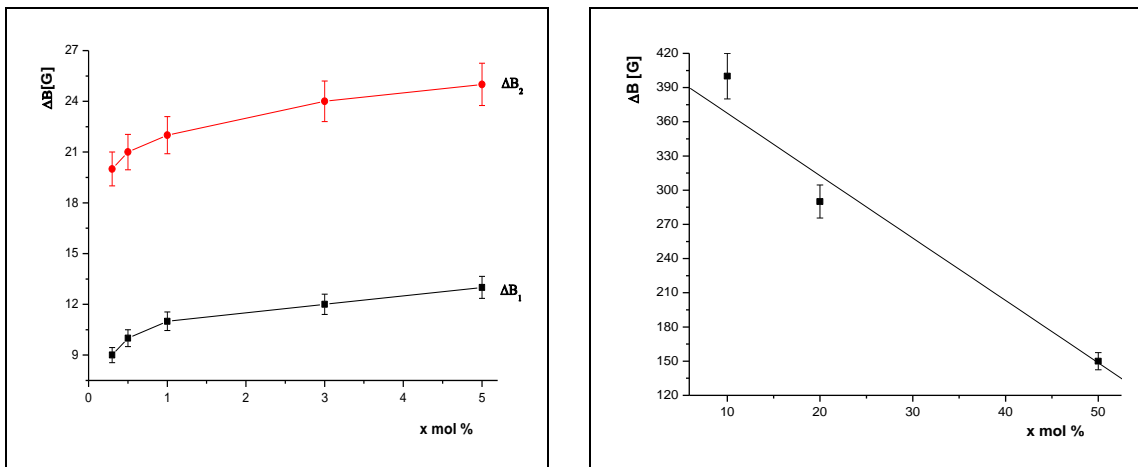


Fig. 5. Composition dependence of the line-width of the first and second hfs-peaks from the parallel absorption (a) and of the broad line characteristic to the cluster formation (b). (The error bars are provided with 5% error limits)

CHAPTER 4

STRUCTURAL STUDIES OF $V_2O_5 - P_2O_5 - Bi_2O_3$ GLASS SYSTEM

$xV_2O_5(100-x)[0.8P_2O_5 \cdot 0.2Bi_2O_3]$ (S_1) and $xV_2O_5(100-x)[0.5P_2O_5 \cdot 0.5Bi_2O_3]$ (S_2) glass systems, with $0 \leq x \leq 50\%$ mol, were prepared and investigated. High purity $(NH_4)_2HPO_4$, Bi_2O_3 and V_2O_5 powders were used as starting materials; melting temperature: $1250^\circ C$ for the first glass system and $1270^\circ C$ for the second glass system; time of melting: 5 min.

It is observed a competition between Bi_2O_3 and P_2O_5 , classical former oxides, on one side and the network modifier, V_2O_5 , on the other side for $xV_2O_5(100-x)[0.5P_2O_5 \cdot 0.5Bi_2O_3]$ glass system. Both Bi_2O_3 and P_2O_5 are network former oxides, but P_2O_5 forms more organized long range structures than Bi_2O_3 .

IR study of $xV_2O_5(100-x)[0.5P_2O_5 \cdot 0.5Bi_2O_3]$ glass system

IR spectra for $xV_2O_5(100-x)[0.5P_2O_5 \cdot 0.5Bi_2O_3]$ glass system, with $0 \leq x \leq 50\%$ mol, are given in figure 6.

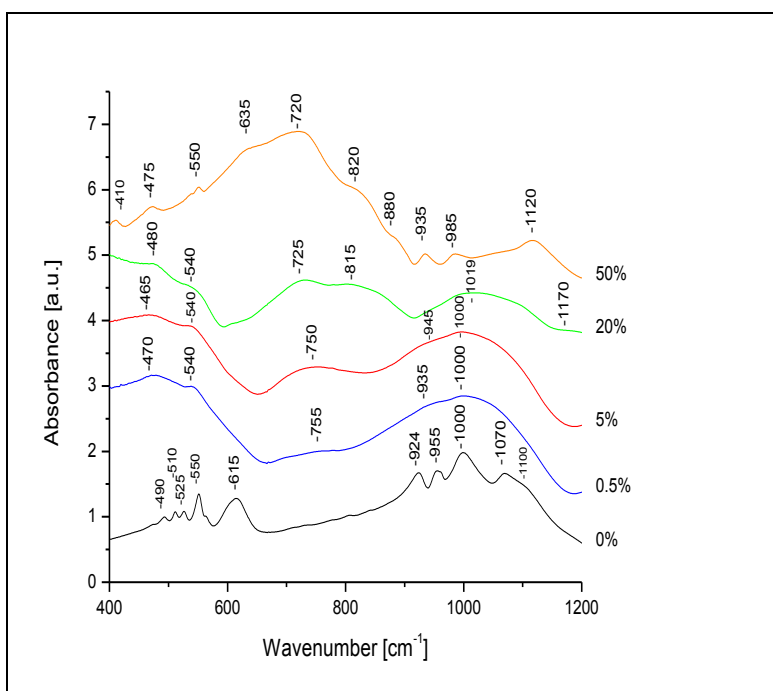


Fig. 6. IR spectra of $xV_2O_5(100-x)[0.5P_2O_5 \cdot 0.5Bi_2O_3]$ glass system

The specific bands for the phosphate-bismuthate network ($x = 0\%$ mol) are situated in the following two regions: $\sim 460 - 650 \text{ cm}^{-1}$ and $\sim 900 - 1150 \text{ cm}^{-1}$. The feature of this spectrum differs from those specific for the phosphate matrix, where three absorption regions are evidenced: $\sim 460 - 520 \text{ cm}^{-1}$, $\sim 690 - 775 \text{ cm}^{-1}$ and $\sim 900 - 1230 \text{ cm}^{-1}$. This means that Bi_2O_3 oxide plays here a network modifier role, leading to the depolymerization of phosphate network and imposes their structural units over the phosphate ones.

The most important bands observed in the low wavenumber region of phosphate-bismuthate network are: $\sim 490 \text{ cm}^{-1}$ and $\sim 510 \text{ cm}^{-1}$, bands may be attributed to stretching vibrations of $\text{Bi} - \text{O}$ bonds in strongly distorted BiO_6 octahedral units; the band from $\sim 525 \text{ cm}^{-1}$ may be also assigned to $\text{Bi} - \text{O}$ bonds bending vibrations in BiO_6 octahedral units; the overlapped vibrations due to $\text{Bi} - \text{O}$ bonds in BiO_6 octahedral units and the harmonics of bending vibrations of $\text{O} = \text{P} - \text{O}$ linkages appears at $\sim 550 \text{ cm}^{-1}$ and the broad absorption from $\sim 615 \text{ cm}^{-1}$ can be attributed to $\text{Bi} - \text{O}^-$ stretching vibrations (of non-bridging oxygen) in BiO_6 octahedral units. In the high wavenumber region, the bands which appear are: the band at $\sim 924 \text{ cm}^{-1}$ is due to the asymmetric stretching $\text{P} - \text{O} - \text{P}$ modes in the linear metaphosphate chain overlapped by $\text{Bi} - \text{O}$ bonds stretching vibrations from BiO_3 pyramidal units; the bands at $\sim 955 \text{ cm}^{-1}$ and $\sim 1000 \text{ cm}^{-1}$ is due to symmetric stretching of $\text{P} - \text{O}^-$ bonds in the PO_3^{2-} groups. The bands appeared at $\sim 1070 \text{ cm}^{-1}$ and $\sim 1100 \text{ cm}^{-1}$ may be attributed to PO_3^{2-} end groups and to $\text{P} - \text{O}^-$ groups (ending chain), respectively.

Visible changes in the IR spectra shape can be observed after increasing V_2O_5 content from 0.5% mol to 20% mol in the studied glasses. There are three absorption bands in the $\sim 500 \text{ cm}^{-1}$, $\sim 750 \text{ cm}^{-1}$ and $\sim 1000 \text{ cm}^{-1}$ region, typical for phosphate network and their assignments are given in papers. This fact may be attributed to the network modifier role of V_2O_5 by depolymerization process of phosphate-bismuth network, acting especially on the Bi_2O_3 network.

Relevant changes, the shift of certain bands and the appearance of other new bands, characteristics to $\text{P} - \text{O} - \text{V}$, $\text{Bi} - \text{O} - \text{V}$ and $\text{V} - \text{O} - \text{V}$ bonds can be observed in the IR spectrum for $x = 50\%$ mol. The bands in $\sim 410 - 635 \text{ cm}^{-1}$ range are due to the lattice vibrations in vanadium oxide network. The band at $\sim 755 \text{ cm}^{-1}$, assigned to the symmetric stretching vibration of $\text{P} - \text{O} - \text{P}$ linkages, is shifted at $\sim 720 \text{ cm}^{-1}$ for high content of V_2O_5 ($x = 50\%$ mol). The bands from $\sim 820 \text{ cm}^{-1}$ and $\sim 880 \text{ cm}^{-1}$ may be attributed to bridge vibrations of the $\text{V} - \text{O} - \text{V}$ lattice and to symmetric vibrations of $\text{V} - \text{O}$ bonds in VO_4 tetrahedral units, respectively. The band

appeared at $\sim 935 \text{ cm}^{-1}$ may be attributed to the polyvanadate (clustered) ions structures. The V = O vibration in isolated VO_5 trigonal bipyramids give rise to the $\sim 985 \text{ cm}^{-1}$ band.

So, we may finally conclude that vanadium atoms link to the non-bridging oxygen of PO_4 and bismuth units, V_2O_5 becoming a network former for high content.

Raman study of $x\text{V}_2\text{O}_5(100-x)[0.5\text{P}_2\text{O}_5 \cdot 0.5\text{Bi}_2\text{O}_3]$ glass system

Raman spectra of the investigated glasses are shown in figure 7. As in the case of IR spectra, Raman scattering bands are also the result of overlapped vibrations due to the matrix former oxides P_2O_5 , Bi_2O_3 and also to the addition of V_2O_5 oxide.

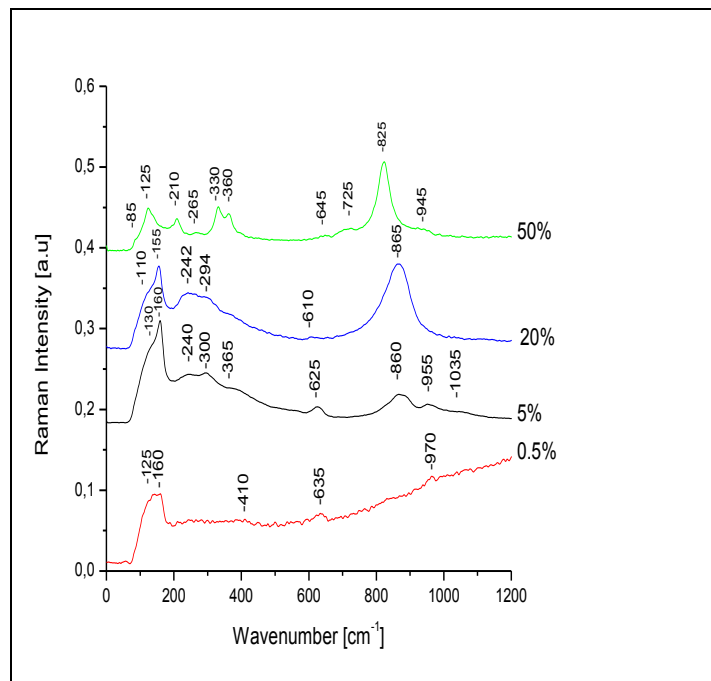


Fig. 7. Raman spectra of $x\text{V}_2\text{O}_5(100-x)[0.5\text{P}_2\text{O}_5 \cdot 0.5\text{Bi}_2\text{O}_3]$ glass system

At low content of V_2O_5 oxide ($x \leq 5\%$ mol), they contain an intense band at $\sim 160 \text{ cm}^{-1}$ with a shoulder at $\sim 130 \text{ cm}^{-1}$ and the following weak bands at $\sim 240 \text{ cm}^{-1}$, $\sim 300 \text{ cm}^{-1}$, $\sim 365 \text{ cm}^{-1}$, $\sim 620 \text{ cm}^{-1}$, $\sim 860 \text{ cm}^{-1}$, $\sim 955 \text{ cm}^{-1}$ and $\sim 1035 \text{ cm}^{-1}$.

The bands from $\sim 130 \text{ cm}^{-1}$ and $\sim 160 \text{ cm}^{-1}$ are an evidence for the existence of BiO_3 and BiO_6 polyhedra in the investigated glass structure. Their intensities decrease with the increasing of V_2O_5 content ($x \geq 20\%$ mol) and the band from $\sim 160 \text{ cm}^{-1}$ disappears for $x = 50\%$ mol when V_2O_5 plays a network former role.

We can also assume that the $\sim 200 - 650 \text{ cm}^{-1}$ spectral region of the Raman spectra appears only due to the bismuth unit vibrations as bridged anion and angularly cation-anion-cation constrained. Thus the weak band from $\sim 300 \text{ cm}^{-1}$ may be assigned to Bi – O vibration. Also, the two Raman bands from $\sim 365 \text{ cm}^{-1}$ and $\sim 625 \text{ cm}^{-1}$ can be attributed to Bi – O – Bi vibrations of BiO_6 octahedral units and to Bi – O stretching vibrations in the distorted BiO_6 octahedral units. The intensity of the last band decreases with the increasing of V_2O_5 content ($x \geq 20\%$ mol).

The appearance of $\sim 1035 \text{ cm}^{-1}$ weak band for $x = 5\%$ mol, due to the symmetric PO_3^{2-} stretching modes, indicates a depolymerization process of the initial metaphosphate chains and therefore, V_2O_5 acts as a strong network modifier for low content.

Band at $\sim 860 \text{ cm}^{-1}$ (for $x = 5\%$ mol) may be assigned to the superposition of symmetric stretching vibration of Bi – O bonds in BiO_3 units with bridge vibrations of V – O – V chains. Its increasing in intensity for $x = 20\%$ mol and shifting to $\sim 825 \text{ cm}^{-1}$ for $x = 50\%$ mol, suggest also the network former role of V_2O_5 at high content.

For low content of V_2O_5 ($x \leq 5\%$ mol), the bismuth units ($\sim 200 - 600 \text{ cm}^{-1}$ region) prevail in the Raman spectra of these glasses. On the other hand, the appearance of an intense band at $\sim 860 \text{ cm}^{-1}$ (for $x \geq 20\%$ mol) suggests the appearance of new structural atomic units with vanadium ions involvement.

EPR study of $x\text{V}_2\text{O}_5(100-x)[0.5\text{P}_2\text{O}_5 \cdot 0.5\text{Bi}_2\text{O}_3]$ glass system

The EPR spectra of this glass system (Fig. 8) did not put in evidence the hyperfine structure typical for isolated vanadyl ions in a C_{4v} symmetry. This fact suggests that for low content of V_2O_5 ($x < 20\%$ mol) both Bi_2O_3 and V_2O_5 induced the depolymerization of the phosphate network, as vanadium ions are not located in isolated positions, but involved in dipole - dipole interactions, leading to the appearance of a broad EPR signal.

For $x = 20\%$ mol the phosphate network has a small tendency of polymerization as the metallic V^{4+} ions are now fixed in some isolated positions and thus leads to the appearance of some weak hyperfine peaks in the EPR spectrum.

By the increasing V_2O_5 content up to $x = 50\%$ mol, P_2O_5 and Bi_2O_3 networks are strongly affected by depolymerization and superexchange interactions prevail between vanadium ions, leading to the widening of the EPR signal.

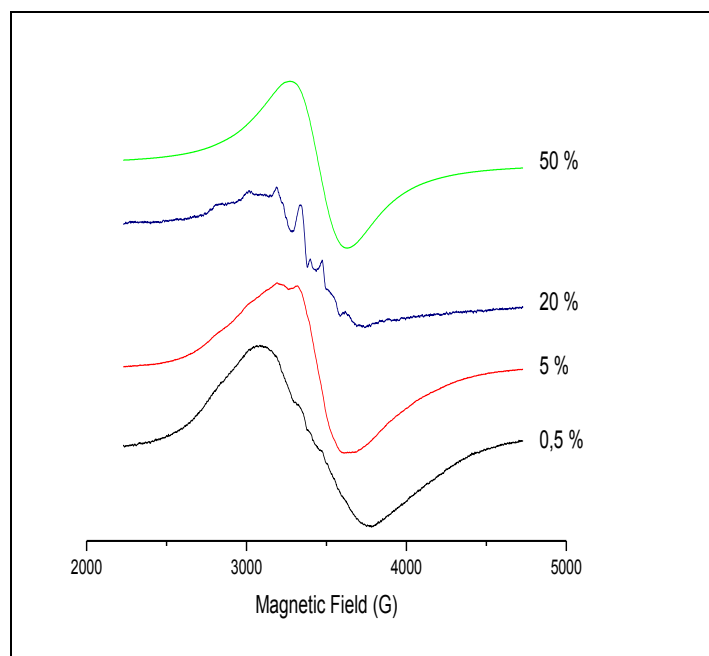


Fig. 8. EPR spectra of $xV_2O_5(100-x)[0.5P_2O_5 \cdot 0.5Bi_2O_3]$ glass system

CHAPTER 5

$V_2O_5 - P_2O_5 - K_2O$ GLASS SYSTEM. ANTIBACTERIAL EFFECT

$xV_2O_5(1-x)[0.8P_2O_5 \cdot 0.2K_2O]$ glass system, with $0 \leq x \leq 50\%$ mol, was prepared and investigated. High purity $(NH_4)_2HPO_4$, K_2CO_3 și V_2O_5 powders were used as starting materials; melting temperature: $1250^\circ C$; time of melting: 5 min.

IR study of $xV_2O_5(100-x)[0.8P_2O_5 \cdot 0.2K_2O]$ glass system

IR absorption spectra for phosphate glasses usually give significant bands in the frequency region $400 - 1100\text{ cm}^{-1}$. According the previous data, V_2O_5 gives in the IR spectra an important band at $\sim 880\text{ cm}^{-1}$ due to V – O vibration in V – O – V chains and at $\sim 1100\text{ cm}^{-1}$ for V = O vibration.

Fig. 9 shows the IR spectra of $xV_2O_5(100-x)[0.8P_2O_5 \cdot 0.2K_2O]$ glass system, with $0 \leq x \leq 50\%$ mol, in the $400 - 1400\text{ cm}^{-1}$ range.

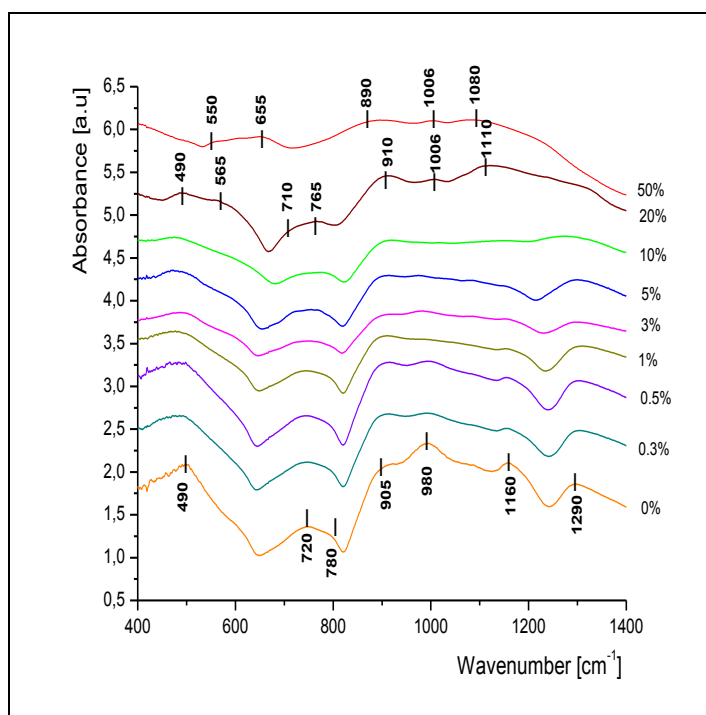


Fig. 9. IR spectra of $xV_2O_5(100-x)[0.8P_2O_5 \cdot 0.2K_2O]$ glass system

The IR spectra of $xV_2O_5(100-x)[0.8P_2O_5 \cdot 0.2K_2O]$ glass system suggest this dual role of vanadium oxide. For low concentration of V_2O_5 ($x \leq 10\%$ mol), the spectra are dominated by the bands belonging to phosphate groups and for high concentration of V_2O_5 ($x \geq 20\%$ mol), the spectra are dominated by the bands belonging to vanadate groups.

Table 2 indicates the values and the bands attribution in the investigated glasses.

Table 2. IR bands assignment for $xV_2O_5(100-x)[0.8P_2O_5 \cdot 0.2K_2O]$ glass system

Wavenumber $\nu[\text{cm}^{-1}]$	Band assignment
~ 490 – 655	Bending vibrations of O – P – O units The lattice vibrations in vanadium oxide network
~ 710 – 780	Stretching vibrations of P – O – P linkages
~ 890 – 910	Asymmetric stretching modes of the P – O – P linkages in linear metaphosphate chain and symmetric vibrations of the V – O bonds of the VO_4 tetrahedra
~ 980 – 1006	Symmetric stretching vibrations in PO_3^{2-} end groups and also in the polivanadate ions formations
~ 1080 – 1160	Symmetric stretching vibrations in P – O groups (chain terminator) and V = O vibrations in the VO_5 tetragonal pyramid
~ 1290	Asymmetric stretching vibrations of P = O bonds

EPR study of $xV_2O_5(100-x)[0.8P_2O_5 \cdot 0.2K_2O]$ glass system

Representative ESR spectra of $xV_2O_5(100-x)[0.8P_2O_5 \cdot 0.2K_2O]$ glass system are given in figure 10.

For low content of V_2O_5 ($x < 10\%$ mol) these spectra show a well resolved hyperfine structure (hfs) typical for vanadyl ions in a C_{4v} symmetry.

EPR parameters for vanadium ions in the studied glasses are given in table 3. The values obtained are in good agreement with other results reported in literature.

Table 3. ESR parameters for V^{4+} ions in $xV_2O_5(100-x)[0.8 P_2O_5 \cdot 0.2 K_2O]$ glass system*

x mol%	g_{\parallel}	g_{\perp}	A_{\parallel} 10^{-4} cm^{-1}	A_{\perp} 10^{-4} cm^{-1}	K	P 10^{-4} cm^{-1}	β_2^2	ϵ_{π}^2
0.3	1.92	2.00	193	79	0.88	133	1.12	0.90
0.5	1.93	1.99	193	77	0.86	135	1.08	0.91
1	1.93	2.00	195	78	0.85	137	1.10	0.90
3	1.93	1.99	197	78	0.84	139	1.08	0.92
5	1.92	2.00	198	77	0.83	140	1.12	0.91

*The error on g values is 0.01 and $1 \cdot 10^{-4} \text{ cm}^{-1}$ on the A values.

For very low content of V_2O_5 oxide ($x \leq 1\text{mol}\%$) the network is dominated by P_2O_5 oxide which has a polymeric structure (organized at long range) and fixes metallic ions in some specific positions, finally determining an isolated distribution species without interaction between paramagnetic ions (V^{4+}).

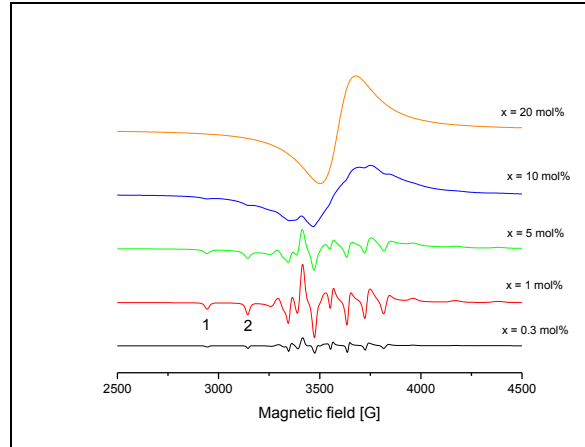


Fig. 10. Representative EPR spectra of $xV_2O_5(100-x)[0.8P_2O_5 \cdot 0.2K_2O]$ glass system

By increasing the V_2O_5 content ($x \leq 10\% \text{ mol}$) this leads to the depolymerization of phosphate network which affects (destroys) isolated distribution mode of metallic ions allowing the appearance of dipole-dipole interactions between them and the linewidth of hfs-lines (peaks) increasing. Dependence of ΔB_1 and ΔB_2 linewidths for the first (1) and second (2) peaks in the parallel absorption band versus vanadium content (Fig. 11) confirm this fact. For this reason, the shape of EPR spectra suggest the network modifier role of V_2O_5 with the depolymerization of the phosphate network.

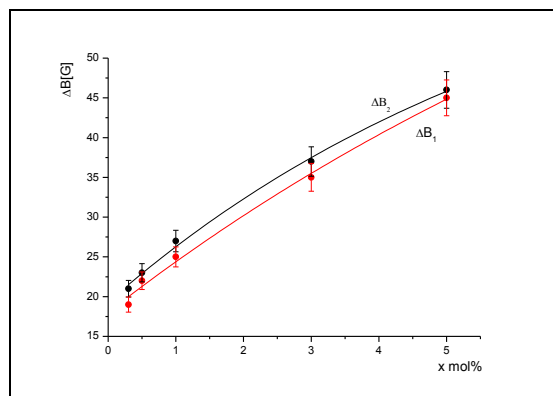


Fig. 11. ΔB_1 and ΔB_2 line widths dependences versus V_2O_5 content
(The error bars are provided with 5 % error limits)

At high content of vanadium oxide ($x \geq 20\%$ mol), the EPR spectra may be regarded as a superposition of two ESR signals, one with a well-resolved hfs typical for isolated VO^{2+} ions and another one consisting in a broad line typical for associated $V^{4+} - V^{4+}$ ions. The number of associated ions increases with the increasing of V_2O_5 content and the presence of superexchange interaction in $V^{4+} - O^{2-} - V^{4+}$ chains appears. This is suggested by the dependence of the broad line ΔB characteristic to the cluster formation in function of V_2O_5 content (Fig. 12). These vanadate structures which isolate the phosphate groups at high V_2O_5 content is in a good agreement with the network former role of vanadium oxide.

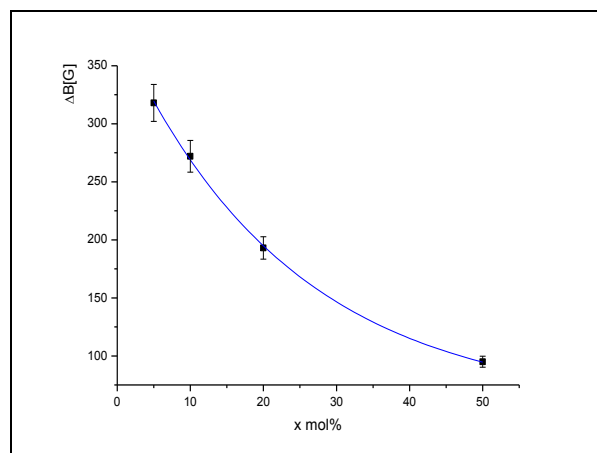


Fig. 12. The dependence of the cluster line (ΔB) with V_2O_5 content
(The error bars are provided with 5% error limits)

Antibacterial effect study of $xV_2O_5(100-x)[0.8P_2O_5 \cdot 0.2K_2O]$ glass system

The vanadium containing system has been tested against gram negative (*E. coli*) and positive (*S. aureus*) bacteria in order to assess its antibacterial activity by plotting the optical density as a function of V_2O_5 content. The efficiency of antimicrobial effect of vanadium incorporated into vitreous system was dependent of its doping content. The optical density (OD) of the samples has been plotted as a function of vanadium concentration in Fig. 13 for the tests conducted in case of *S. aureus* and in Fig. 14 in case of *E. coli* strain.

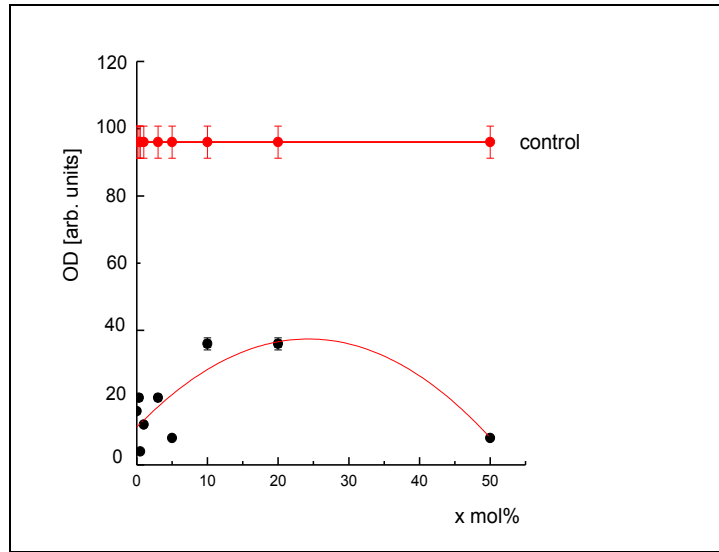


Fig.13. Optical density versus $xV_2O_5(100-x)[0.8 P_2O_5 \cdot 0.2 K_2O]$ glasses containing *S. aureus* bacteria (The error bars are provided with 5 % error limits)

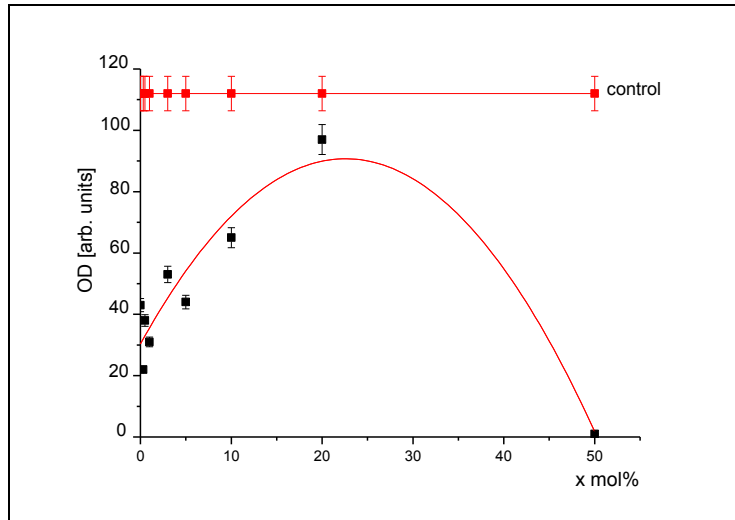


Fig.14. Optical density versus $xV_2O_5(100-x)[0.8 P_2O_5 \cdot 0.2 K_2O]$ glasses containing *E. coli* strains (The error bars are provided with 5 % error limits)

From Fig. 13, 14 we can observe a stronger inhibitory effect on Gram-negative bacteria (*E. coli*), than the Gram-positive (*S. aureus*). The strongest effects occur at low concentrations ($x < 10\%$ mol) as well as at high content ($x > 30\%$ mol) of V_2O_5 . The antibacterial activity of the investigated system presents the same tendency for both Gram-positive and Gram-negative strains.

The highest antimicrobial effect can be correlated with atomic dispersion (isolated) of vanadium ions ($x < 5\%$ mol) and the lowest effect for vanadium ions involved in the clusterization process. This process is prevalent for a content of V_2O_5 between 10 and 30% mol, when the depolymerization effect produced on the potassium-phosphate network is maximum, as well as the clustering process. The atomic dispersion (isolated ions) of vanadium ions at high concentrations of V_2O_5 ($x \geq 30\%$ mol%) is due to its unconventional former effect, vanadium ions being involved in new P – O – V, V – O – V linkages.

CHAPTER 6

$P_2O_5 - BaO - K_2O$ GLASS SYSTEM. THERMOLUMINESCENCE PROPERTIES

$0.5P_2O_5 - xBaO - (0.5-x)K_2O$ glass system, with $0 \leq x \leq 0.5$, was prepared and investigated. High purity $(NH_4)_2HPO_4$, $BaCO_3$ și K_2CO_3 powders were used as starting materials; melting temperature: $1200^\circ C$; time of melting: 1 hour.

IR study of $0.5P_2O_5 - xBaO - (0.5-x)K_2O$ glass system

IR spectra of $0.5P_2O_5 - xBaO - (0.5-x)K_2O$ glass system, with $0 \leq x \leq 0.5$, are given in figure 15.

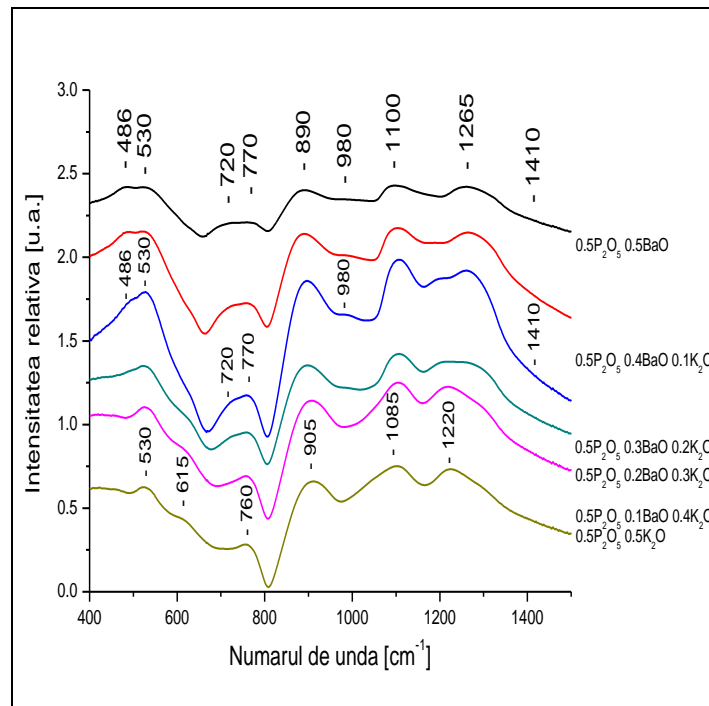


Fig. 15. IR spectra of $0.5P_2O_5 - xBaO - (0.5-x)K_2O$ glass system

Fig. 15 shows that the specific IR bands of the studied glasses are situated in the following regions: $\sim 500\text{ cm}^{-1}$, $\sim 720 - 770\text{ cm}^{-1}$ and $\sim 890 - 1410\text{ cm}^{-1}$.

For the studied glasses, the assignments of the detected absorption bands are summarized in table 4.

Table 4. IR bands assignment for $0.5\text{P}_2\text{O}_5 - x\text{BaO} - (0.5-x)\text{K}_2\text{O}$ glass system

Wavenumber $\nu[\text{cm}^{-1}]$	Band assignment
~ 486	Bending vibrations of O – P – O units
~ 530	Harmonics of bending vibrations of P = O bond
~ 615	Harmonics of stretching vibrations of O = P – O linkages
$\sim 720 - 770$	Symmetric stretching vibrations of P – O – P linkages
$\sim 890 - 905$	Asymmetric stretching modes of the P – O – P linkages in linear metaphosphate chain
~ 980	Symmetric stretching vibrations in PO_4^{3-} groups
$\sim 1085 - 1100$	Symmetric stretching vibrations in PO_2^- groups
$\sim 1220 - 1265$	Asymmetric stretching vibrations of P = O bonds
~ 1410	Symmetric stretching vibrations of P = O bonds

The frequency changes of P – O – P bands of the studied glasses by increasing the K_2O content is in good agreement with the breaking of the P – O – P phosphate chains, when K_2O plays the modifier network role.

Raman study of $0.5\text{P}_2\text{O}_5 - x\text{BaO} - (0.5-x)\text{K}_2\text{O}$ glass system

Raman spectra (Fig. 16) of the studied phosphate glasses contain two important regions at $\sim 700 \text{ cm}^{-1}$ and $\sim 1150 \text{ cm}^{-1}$. Except these two regions we can observe other bands under $\sim 600 \text{ cm}^{-1}$ in the Raman spectra of these phosphate glasses.

The presence of Ba^{2+} and K^+ ions in the phosphate network is manifesting by shifting and changing intensity of some characteristic bands of P – O groups. This fact is possible by changing the covalence angle and length for P – O chains and by favoring the appearance or disappearance of some structural phosphate groups.

Band assignment for different vibration bands in the Raman spectra of $0.5\text{P}_2\text{O}_5 - x\text{BaO} - (0.5-x)\text{K}_2\text{O}$ glass system is indicates in table 5.

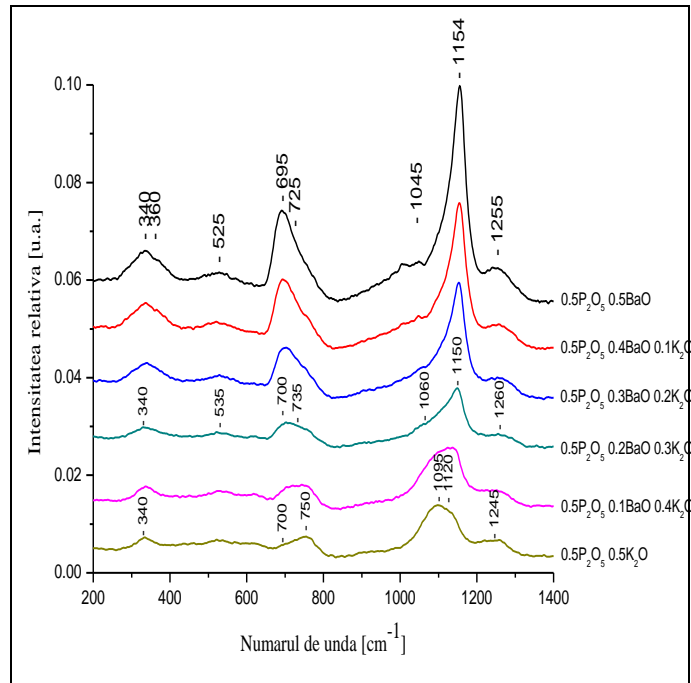


Fig. 16. Raman spectra of $0.5\text{P}_2\text{O}_5 - x\text{BaO} - (0.5-x)\text{K}_2\text{O}$ glass system

Table 5. Raman bands assignment for $0.5\text{P}_2\text{O}_5 - x\text{BaO} - (0.5-x)\text{K}_2\text{O}$ glasses

Wavenumber $\nu[\text{cm}^{-1}]$	Band assignment
~ 340 ~ 360	Bending vibrations in phosphate chains Bending vibrations in PO_3^{2-} groups
~ 525 – 535	Stretching vibrations due to the cations and chain structures movement
~ 695 – 750	Symmetric stretching vibrations of P – O – P linkages
~ 1045 – 1095	Symmetric stretching vibrations in P – O groups and Symmetric stretching vibrations in PO_3^{2-} groups
~ 1120 – 1154	Symmetric stretching vibrations of O – P – O linkages
~ 1245 – 1260	Asymmetric stretching vibrations of P = O bonds

Thermoluminescence study of $0.5\text{P}_2\text{O}_5 - x\text{BaO} - (0.5-x)\text{K}_2\text{O}$ glass system

The glow curves of $0.5\text{P}_2\text{O}_5 - x\text{BaO} - (0.5-x)\text{K}_2\text{O}$ glass system (Fig. 17) contain overlapping thermoluminescence peaks observed in the case of $0.5\text{P}_2\text{O}_5 \cdot 0.5\text{BaO}$ and $0.5\text{P}_2\text{O}_5 \cdot 0.5\text{K}_2\text{O}$ glasses.

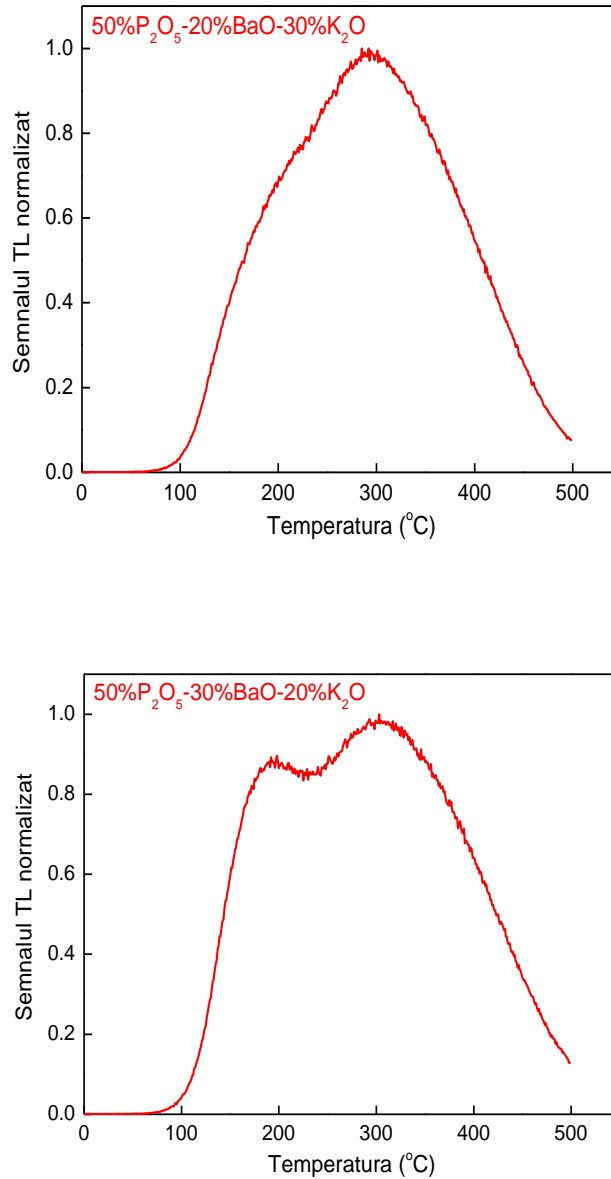


Fig. 17. Glow curves of $0.5\text{P}_2\text{O}_5 - x\text{BaO} - (0.5-x)\text{K}_2\text{O}$ glass system

It was observed that the presence of both Ba^{2+} and K^+ modifier ions leads to the generation of thermoluminescence phenomena. In the case of barium doped glasses a linear dependence of the dose in function of the thermoluminescence emission occurs in the UV region, a linear dependence higher than the saturation limit of the most traditional metals. A very good linear dependence of the integral of thermoluminescence signal in function of the irradiation dose can be observed for both dosimetric peaks typical for $0.5P_2O_5 \cdot 0.5BaO$ glass system up to 50 Gy.

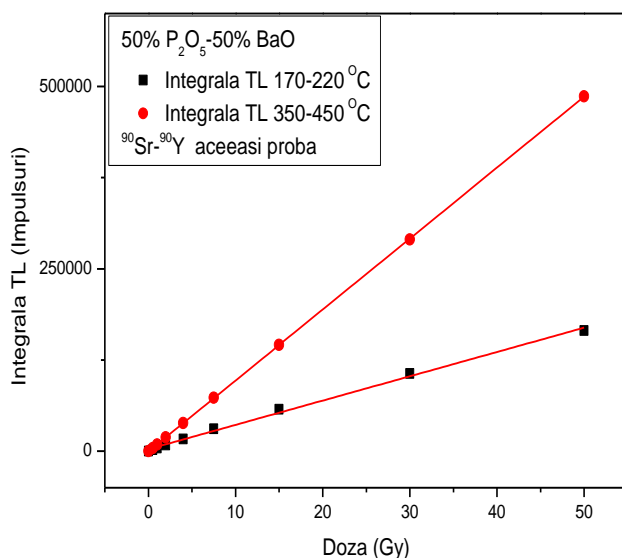


Fig. 18. Integral of thermoluminescence signal in function of the irradiation dose for $0.5P_2O_5 \cdot 0.5BaO$ glass system

CONCLUSIONS

- Five binary phosphate glass systems containing Ba, Bi and K ions doped with various concentrations of V_2O_5 were prepared and studied:

S1: $xV_2O_5(100-x)[0.8P_2O_5 \cdot 0.2BaO]$, cu $0 \leq x \leq 50$ mol%;

S2: $xV_2O_5(100-x)[0.8P_2O_5 \cdot 0.2Bi_2O_3]$, cu $0 \leq x \leq 50$ mol%;

S3: $xV_2O_5(100-x)[0.5P_2O_5 \cdot 0.5Bi_2O_3]$, cu $0 \leq x \leq 50$ mol%;

S4: $xV_2O_5(100-x)[0.8P_2O_5 \cdot 0.2K_2O]$, cu $0 \leq x \leq 50$ mol%;

S5: $0.5P_2O_5 - xBaO - (0.5-x)K_2O$, cu $0 \leq x \leq 0.5$.

- The main goal of the present study was that to reveal the local structure and network modifications induced by variable concentrations of modifier ions. New information regarding thermoluminescence properties or antibacterial properties of some of the investigated glasses was also obtained.

- The investigation methods used in this study were IR and Raman spectroscopy, EPR (electron paramagnetic resonance), thermoluminescence measurements and microbiological tests to evidence the antimicrobial character of some of the investigated glasses.

- In the case of vanadium doped glasses, the increase of V_2O_5 content induced an increase of the structural disorder under the form of network depolymerization up to 10 mol%.

- IR spectra of all investigated glass systems proved to be more consistent in showing the structural network modifications then the Raman once.

- For high V_2O_5 content ($x \geq 20$ mol%), the reduction of the bonding forces between P and O atoms leads to the appearance of non-bridging oxygen atoms involved in new V – O – V or P – O – V bonds, suggesting the network former role of V_2O_5 oxide.

- Both IR and Raman spectra revealed the dual role of V_2O_5 , that of network modifier at low concentration ($x \leq 10$ mol%) and that of network former at high concentration ($x \geq 20$ mol%).

- EPR spectra of S₁, S₂ and S₄ systems have shown the change of the spectral shape with the increase of V_2O_5 content from one typical for V^{4+} ions to a wide line typical for

clustered ions. For $x \leq 10$ mol%, dipole-dipole interactions prevail between V^{4+} ions, while for $x \geq 20$ mol% superexchange interactions become prevalent.

- For S_3 system, it was observed a competition between Bi_2O_3 and P_2O_5 , as classical former oxides on one side and the network modifier V_2O_5 , on the other side. Both Bi_2O_3 and P_2O_5 are network former oxides, but P_2O_5 forms more organized long range structures than Bi_2O_3 .

- In IR spectra of $[0.5P_2O_5 \cdot 0.5Bi_2O_3]$ glass matrix of S_3 system, Bi_2O_3 acts as a network modifier, imposing its own network over the phosphate one. For low V_2O_5 content ($x \leq 10$ mol%), the depolymerization is made especially on the Bi_2O_3 component. For high V_2O_5 content ($x \geq 20$ mol%), vanadium ions connect with the non-bridging oxygen ions making new $V - O - V$, $P - O - V$, $Bi - O - V$ chains, suggesting its forming role.

- EPR spectra of S_3 glass system did not put in evidence the hyperfine structure typical for isolated vanadyl ions in C_{4v} symmetry. For low content of V_2O_5 ($x < 20$ mol%), V^{4+} ions are involved in dipole - dipole interactions, leading to the appearance of a broad EPR signal. For $x = 20$ mol%, the phosphate network has a small tendency of polymerization and for high content of V_2O_5 ($x = 50$ mol%), superexchange interactions prevail between vanadium ions, leading to the widening of the EPR signal.

- For S_5 system, the characteristic bands in IR and Raman spectra were attributed to different vibrations in Q^n structural units. The presence of K^+ and Ba^{2+} modifier ions changes the covalence angle in $P - O$ chains and favors the appearance or the disappearance of different structural units.

- Thermoluminescence measurement made for S_5 glass system have shown that the presence of both Ba^{2+} and K^+ modifier ions leads to the generation of thermoluminescence phenomena. In the case of barium doped glasses, a linear dependence of the dose in function of the thermoluminescence emission in the UV region was observed, a dependence higher than the saturation limit of the most traditional metals.

- Antibacterial test were made for S_4 glass system containing potassium ions. The efficiency of antimicrobial effect of vanadium incorporated into vitreous system was dependent of its doping content. The highest antimicrobial effect can be correlated with atomic dispersion (isolated) of vanadium ions ($x < 5$ mol%) and the lowest effect for vanadium ions involved in the clusterization process (associated ions).

SELECTED REFERENCES

- [1] P. Baltă, *Tehnologia sticlei*, Ed. Didactică și Pedagogică, București (1984)
- [2] I. Ardelean, *Introducere în studiul materialelor oxidice cu structură vitroasă*, Ed. Napoca Star, Cluj-Napoca (2002)
- [3] J. E. Garbarczyk, M. Wasiucionek, P. Jozwiak, L. Tykarski, J. L. Nowinski, *Solid State Ionics* 154-155, 367 (2002)
- [4] G. Tricot, L. Montagne, L. Delevoye, G. Palavit, V. Kostoj, *J. Non-Cryst. Solids* 345-346, 56 (2004)
- [5] T. Iliescu, D. Maniu, S. Pînzaru, R. Grecu, S. Aștilean, *Aplicații ale spectroscopiei vibraționale*, Casa Cărții de Știință, Cluj-Napoca (2002)
- [6] A. Magdaș, O. Cozar, V. Chiș, I. Ardelean, N. Vedeanu, *Vibrational Spectroscopy* 48, 251 (2008)
- [7] L. David, C. Crăciun, O. Cozar, V. Chiș, *Rezonanță electronică de spin-principii, metode, aplicații*, Presa Univ. Clujeană (2001)
- [8] O. Cozar, V. Grecu, V. Znamirovski, *Rezonanță electronică de spin pe complecși metalici*, Ed. Academiei Române, București (2001)
- [9] V. E. C. Linda, M. Teixeira, *Effect of thermal treatments on different commercial glasses for use of radiation detectors*, I.R.P.A., Spain (2004)
- [10] R. K. Brow, *J. Non-Cryst. Solids*, 263-264, 1 (2000)
- [11] P. Y. Shih, J. Y. Ding, S. Y. Lee, *Mater. Chem. Phys.* 80, 391 (2003)
- [12] H. Doweidar, Y. M. Moustafa, K. El-Egili, I. Abbas, *Vib. Spectrosc.* 37, 91 (2005)
- [13] P. Bergo, S. T. Reis, W. M. Pontuschka, J. M. Prison, C. C. Motta, *J. Non-Cryst. Solids* 336, 159 (2004)
- [14] I. Ardelean, S. Cora, *J. Optoelectron. Adv. Mater.* 12/2, 239 (2010)
- [15] M. A. Karakassides, A. Saranti, I. Koutselas, *J. Non-Cryst. Solids* 347, 69 (2004)
- [16] I. Ardelean, O. Cozar, N. Vedeanu, D. Rusu, C. Andronache, *J. Mater. Sci.: Mater. Electron.* 18, 963 (2007)
- [17] A. Magdaș, O. Cozar, I. Ardelean, L. David, *J. Optoelectron. Adv. Mater.*, 9(3), 730 (2007)

- [18] N. Vedeanu, R. Stănescu, S. Filip, I. Ardelean, O. Cozar, *J. Non-Cryst. Solids* 358, 1881-1885 (2012)
- [19] R. Stănescu, N. Vedeanu, L. Țibre, I. Ardelean, O. Cozar, *4th Conference on Advanced Spectroscopies on Biomedical and Nanostructured Systems*, Cluj-Napoca, România, 134 (2011)
- [20] R. Stănescu, N. Vedeanu, I. Ardelean, O. Cozar, *Physics Conference TIM-12*, Timișoara, România, 105 (2012)
- [21] N. Vedeanu, O. Cozar, R. Stănescu, I. B. Cozar, I. Ardelean, *J. Mol. Structure* 1044, 323-327 (2013)
- [22] R. Stănescu, N. Vedeanu, L. Țibre, I. Ardelean, *Studia Universitatis Babeș-Bolyai, Physica LV*, 2, 115-122 (2010)
- [23] R. Stănescu, N. Vedeanu, I. B. Cozar, A. Magdaș, *AIP Conference Proceedings of the Isotopic and Molecular Processes (PIM)*, Cluj-Napoca, România, 1565, 122-125 (2013)
- [24] N. Vedeanu, I. B. Cozar, R. Stănescu, R. Ștefan, D. Vodnar, trimisă spre publicare la *Journal of Material Science : Materials in Medicine* (2014)
- [25] N. Vedeanu, R. Stănescu, O. Cozar, I. Ardelean, *8th General Conference of Balkan Physical Union*, Constanța, România, 136 (2012)
- [26] N. Vedeanu, R. Stănescu, A. Magdaș, C. Voica, *19th International Mass Spectrometry Conference*, Kyoto, Japonia, 46 (2012)

ACKNOWLEDGEMENTS

At the end of my PhD study, I would like to express my gratitude to the people who helped me all these years.

I express my deepest gratitude to my scientific supervisor, Prof. dr. Onuc Cozar, for the opportunity to do this PhD research in his working group. I thank him for the excellent guidance and for his trust in me all these years.

I would like also to express my gratitude to Assoc. prof. dr. Nicoleta Vedeanu, for her permanent collaboration in publishing the scientific results of this PhD research and for her useful scientific advice and to Prof. dr. Ioan Ardelean, for his encouragement, moral support and practical help during my PhD stage.

I thank also to all the members of Biomolecular Physics Department, especially to Prof. dr. Viorica Simon, Prof. dr. Leontin David and Assoc. prof. dr. Liviu Dărăban, for their help and collaboration all these years.

Many thanks to Lecturer dr. Alida Timar Gabor, from Faculty of Environmental Science and Engineering, Cluj-Napoca for her assistance in the achievement of thermoluminescence measurements and for our useful discussions.

Cluj-Napoca, iulie 2014

Ramona Stănescu